J Mater Sci (2007) 42:9154–9162
DOI 10.1007/s10853-007-1928-8

Evolution of the electronic structure and properties of neutral and charged arsenic clusters

Ling Guo

Received: 18 March 2007 / Accepted: 8 June 2007 / Published online: 28 July 2007

Abstract Geometrical and electronic properties of As_n ($n = 2$–15) neutrals, cations and anions have been investigated using the density functional method of B3LYP. Berny structural optimization and frequency analyses are performed with the basis of 6-311 + G(d) for both neutrals and charged ions. The total energies of these clusters are then used to study the evolution of their binding energy, relative stability, and electronic properties as a function of size. The geometries are found to undergo a structural change from two dimensional to three-dimensional when the cluster contains four atoms. The geometrical changes are companied by corresponding changes in the nearest-neighbor distances and coordination numbers. In the whole size range, both ionization potential and electron affinity have the tendency of decrease when the number of As units in the cluster increases. The stability of clusters exhibits strong even-odd alternations with several magic numbers. The neutral As_n clusters are found to be even-numbered with local maxima at $n = 2$ and 4, while the cationic and anionic clusters are preferentially odd-numbered with As_3^+, As_5^+, and As_5^- being the most stable ions according to the calculated results of the both energy gain and electronic properties.

Introduction

The V clusters have been the topic of many experimental and theoretical studies [1–9]. They have been studied widely as components of organometallic and other molecular [10–12]. Besides the famous phosphorus, arsenic is known to form a wide range of homoatomic clusters and arsenic, in the form of clusters, has displays endless varieties as well as structures. Up to the present the structure and electronic state of neutral As_n ($n = 2$–6) clusters have been well theoretically understood [1, 2, 5]. However, experiments by photo ionization and photoelectron spectroscopy have found the evidence for the existence of positively [3] and negatively [4] charged clusters.

But, compared to neutrals much fewer strict theoretical calculations for charged clusters have been reported. The electronic state and relative stability of these charged As_n clusters remain unclear. Chi et al. [5] explain the structure and frequency of As_n^- ($n = 2$–5) using the combination of three density functional theory approaches: the local-spin-density approximation Slater-VWN functional [13], the gradient-correction Becke88-LYP functional [14] and the hybrid Becke3-LYP functional [15]. Nevertheless more accurate theoretical calculation, frequency analyses and a stability check are required to confirm this explanation. In the present study, with standard B3LYP/6-311 + G(d) method we extend density functional calculations to As_n ($n = 2$–15) anions and cations in order to determine their ground state geometry and their relative stabilities. The charged-induced structural changes in these anions will be discussed.

In addition, we examine, critically, the available experimental data in arsenic clusters as a function of cluster size and compare these with our first principles calculations of the equilibrium geometries and total energies of neutral, positively, and negatively charged clusters containing up to 15 atoms. We have studied the evolution of their atomic structure, coordination number, interatomic distance, binding energy, vertical and adiabatic ionization potential and electron affinities. Comparison of these results with

---

L. Guo (✉)
School of Chemistry and Material Science, Shanxi Normal University, Linfen 041004, China
e-mail: gl-guoling@163.com

experiment and previous theories provides a unique perspective of the evolution of cluster properties.

Since, like the alkalies, the electronic structure of bulk arsenic is free-electronlike, it is expected that arsenic clusters can also be studied by applying simple models. The model that has been most successful in describing the electronic structure of alkali metal clusters is the jellium model [16] where one assumes that the atomic arrangements in the cluster are not very important in describing their electronic structure. One can, thus, approximate the cluster by a spherical distribution of positive ion charge to which the valence electrons respond. Such a description gives rise to electronic shells where the quantum numbers order as $1s^2$, $1p^6$, $1d^{10}$, $2s^2$, $1f^{14}$, $2p^6$.... Thus, clusters with 2, 8, 20, 40,... electrons can close $1s^2$, $1p^6$, $2s^2$, $2p^6$....shells, respectively, and in analogy with nuclear shell structure should be very stable. Neutral alkali metal clusters containing 2, 8, 20, 40... atoms, therefore, should exhibit pronounced stability. Similarly positively charged alkali clusters containing 3, 9, 21, 41... atoms should also be very stable [17]. That this is exactly what was observed experimentally [16, 18] has given tremendous credibility to this simple model.

In the next section we discuss briefly our methodology. The results are discussed in section "Results and discussions". Last section contains a summary of our conclusions.

Methodology

The B3LYP-DFT/6-311 + G(d) method has been employed to optimize the geometries of As_n neutrals and charged ions. Frequency analyses are performed at the same theoretical level to check whether the optimized structures are transition states or true minima on the potential energy surfaces of corresponding clusters. The choice of the hybrid Becke-LYP [15] functional has been fully justified for As_n cluster studies due to the fact that it is an ab initio tool and it includes the electron correlation effect which has been found necessary for arsenic clusters at relatively low computational cost. Electronic properties of these optimized structures including the relative orbital and total energies, I.P.s, and E.A.s are calculated with the same basis sets. The initial input structures are taken either from published results or arbitrarily constructed and fully optimized via the Berny algorithm. Symmetry constrains are removed whenever imaginary frequencies are found. All calculations were carried out using the GAUSSIAN 98 program [19].

In this paper we are concerned with the stability and properties of neutral, cationic (single positive charged), and anionic (single negative charged) clusters. Geometry optimization for all these charged states and two different spin multiplicities were carried out for each of the arsenic clusters containing 2–15 atoms. In total, this amounted to optimizing $14 \times 2 \times 3 = 84$ separate geometries. The results of this optimization are discussed in the following section.

Results and discussions

The past experimental studies on arsenic clusters can be broadly divided into three categories depending upon the prosperities they are designed to investigate. (1) The relative stability of clusters and the existence of magic numbers (i.e., clusters with unusual stability) are probed through time-of-flight mass spectrometry. (2) The electronic structure is probed through measurements of ionization potential, electron affinity, and dipole polarizability. (3) The chemistry of the clusters is studied through their interaction with reagent molecules. We will comment on some of these experiments during the course of our discussion.

Equilibrium geometries, nearest-neighbor distances, and coordination numbers

The starting point in any description of cluster properties is their geometrical structure. Unfortunately, there is no experimental technique that can provide directly information on cluster geometry. The only method that enables determination of cluster geometries at present is, thus, based on theoretical calculations. Unfortunately, the calculated geometries depend on the level of the theory. The better the theory, the smaller the size of the cluster it can handle. The correctness of the geometries determined theoretically can only be established by comparing calculated properties of these clusters with experiment. We believe that we have identified the equilibrium geometries of arsenic clusters containing up to 15 atoms correctly. This belief is based on our ability to explain the mass ion intensity, ionization potentials, and electron affinities for all clusters studied consistently and quantitatively.

The optimized geometric symmetries, electronic state and their total energies of ground states of neutral and charged As_n (n = 2–15) clusters are all listed in Table 1. Their corresponding vibrational frequencies (cm^{-1}) are listed in Table 2. The ground-state structures obtained for some small neutrals and charged (cationic as well as anionic) clusters are identical to those accepted in published references for As_n. The ground-state structures of both neutral and charged arsenic clusters containing 2–15 atoms are all illustrated in Fig. 1. These structures have been confirmed to have no imaginary frequencies and

Table 1 The optimized ground-state structures and total energies E_t (hartree/particle) at B3LYP/6-311 + G(d) level

Cluster	Symmetry	State	E_t	Cluster	Symmetry	State	E_t
As_2	$D_{\infty h}$	$^1\Sigma_g$	–4471.7738	As_9	C_s	$^2A''$	–20123.1351
As_2^+	$D_{\infty h}$	$^2\Sigma_g$	–4471.3976	As_9^+	D_{2d}	$^1A_1$	–20122.8984
As_2^-	$D_{\infty h}$	$^2\Pi_u$	–4471.8084	As_9^-	C_s	$^1A'$	–20123.2446
As_3	$D_{\infty h}$	$^2\Pi_u$	–6707.6117	As_{10}	C_s	$^1A'$	–22359.0657
As_3^+	D_{3h}	$^1A_1'$	–6707.3975	As_{10}^+	C_s	$^2A''$	–22358.7915
As_3^-	D_{3h}	$^3A_1'$	–6707.7303	As_{10}^-	C_s	$^2A''$	–22359.1530
As_4	T_d	$^1A_1$	–8943.6233	As_{11}	C_s	$^2A'$	–24594.9705
As_4^+	C_{2v}	$^2B_2$	–8943.2946	As_{11}^+	C_s	$^1A'$	–24594.7180
As_4^-	C_{2v}	^2A	–8943.6455	As_{11}^-	C_s	$^1A'$	–24595.0678
As_5	C_{2v}	$^2B_1$	–11179.4926	As_{12}	D_{3d}	^1A_g	–26830.8971
As_5^+	C_{4v}	$^1A_1$	–11179.2460	As_{12}^+	D_{3d}	^2B_g	–26830.6226
As_5^-	D_{5h}	$^1A_1'$	–11179.6071	As_{12}^-	D_{3d}	^2B_u	–26830.9653
As_6	D_{3h}	$^1A_1'$	–13415.4084	As_{13}	C_s	$^2A''$	–29066.7423
As_6^+	C_{2h}	^2A_g	–13415.1126	As_{13}^+	C_1	^1A	–29066.5054
As_6^-	C_{2v}	$^2A_2$	–13415.4874	As_{13}^-	C_s	$^1A'$	–29066.8708
As_7	C_{2v}	$^2B_1$	–15651.3199	As_{14}	C_s	$^1A'$	–31302.7051
As_7^+	C_{2v}	$^1A_1$	–15651.0720	As_{14}^+	C_s	$^2A''$	–31302.4355
As_7^-	C_{2v}	$^1A_1$	–15651.4184	As_{14}^-	C_s	$^2A'$	–31302.7507
As_8	C_{2v}	$^1A_1$	–17887.2438	As_{15}	C_s	$^2A'$	–33538.5883
As_8^+	C_s	$^2A'$	–17886.9475	As_{15}^+	C_s	$^1A'$	–33538.3347
As_8^-	C_s	$^2A''$	–17887.3154	As_{15}^-	C_s	$^1A'$	–33538.6995

therefore are true minima. For cations and anions, the ground-state structures are either relaxed within the geometries of corresponding neutrals or distorted into new structures with lower energies and much lower symmetries due to Jahn-Teller distortions.

The electronic state is $^1\Sigma_g$ for the neutral As_2 cluster, and $^2\Sigma_g$ and $^2\Pi$ for cation and anion. The optimized As_2 bond length of 2.111 Å and vibrational frequency of 431 cm^{-1} compare favorably with the experimental value of 2.103 Å and 430 cm^{-1} [22]. For the cationic case, the ionize electron comes out from a bonding orbital predicting its instability relative to the neutral monomer by 10.24 eV. It is also manifested in a decrease of the frequency value (401 cm^{-1} compare to 430 cm^{-1}) indicating that the bond in cationic state is weaker than the corresponding one in the neutral molecule. The anion is found to be 0.94 eV more stable than the neutral one. This is consistent with the fact that the lowest unoccupied molecular orbital (LUMO) of the neutral monomer has the bonding character and is occupied by the additional electron in the anionic cluster. The calculated As_2^- bond length of 2.211 Å also compare favorably with the experimental value of 2.239 Å [4]. Both As_3^+ and As_3^- take equilateral triangle (D_{3h}) as their ground state, while the neutral cluster adopts linear structure ($D_{\infty h}$, $^2\Pi_u$) as its global minimum. For the neutral As_3, the frequencies of 251 and 349 cm^{-1} compare very well with the calculated results of 259 and 349 cm^{-1} [5]. The arsenic tetramer has the tetrahedral (T_d) structure. The additional electron in the anion, however, results in a Jahn-Teller distortion that is so large that the As_4^- considers the C_{2V} structure as its ground state. Different from its neutral and anionic cluster, the cationic As_4^+ is C_{2v} ($^2B_2$) in symmetry. The global minimum of As_5^+ is a square pyramid (C_{4v}, $^1A_1$), while anion As_5^- is a planar pentagonal structure with symmetry of D_{5h} ($^1A_1'$). The two strongest vibrational frequencies of 104, 155, 245 and 272 cm^{-1} are in agreement with the calculated values of 109, 161, 256, and 280 [5]. Different from its charged cluster, the neutral As_5 cluster is a tetrahedral As_4 structure with a twofold atom bond to it. Removing an electron from the triangular prism of As_6 (D_{3h}, $^1A_1'$) produces a cationic As_6^+ with C_{2h} (^2A_g) symmetry which has the different geometry as the neutral, adding one electron to neutral As_6 results in a cuneane anionic As_6^- (C_{2v}). As_7^+ takes a square-face-capped triangle prism (C_{2v}, $^1A_1$) as its ground-state structure. While As_7^- is derived from a boat-shape As_6 by the adding of one two-fold atom, which has the same geometry as the neutral. The lowest-energy structure of As_8 is a cuneane structure with the symmetry of C_{2v} ($^1A_1$), which is different from the previous work published on Ref. [23]. I optimize their structure using the B3LYP/6-311 + G(d) level and found that my structure is the lowest energy structures. And the

Table 2 The vibrational frequencies (cm^{-1}) for the ground states of neutral and charged As$_n$ (n = 2–15) clusters

Cluster	This theory	Experimental and other theory
As$_2$	431	460 [2] 430 [20]
As$_2^+$	401	
As$_2^-$	354	372 [5]
As$_3$	251, 349	259 [5] 349 [5]
As$_3^+$	256, 356	
As$_3^-$	221, 309	220 [5] 329 [5]
As$_4$	194, 248, 335	200.8 [21] 251.0 [21] 342.0 [21] 197.8 [20] 251.6 [20] 341.7 [20]
As$_4^+$	121, 160, 173, 243, 296,	
As$_4^-$	113, 162, 209, 221, 233, 311	174 [5] 227 [5] 316 [5]
As$_5$	69, 134, 186, 198, 202, 232, 240, 244, 299	71 [5] 139 [5] 195 [5] 208 [5] 242 [5] 251 [5] 312 [5]
As$_5^+$	126, 131, 171, 225, 259, 217, 290	
As$_5^-$	104, 155, 245, 269, 272	109 [5] 161 [5] 256 [5] 280 [5]
As$_6$	80, 122, 191, 209, 222, 236, 273, 289	
As$_6^+$	5, 34, 45, 53, 59, 140, 215, 219, 238, 251, 346	
As$_6^-$	48, 90, 139, 144, 165, 173, 195, 218, 222, 225, 272, 286	
As$_7$	49, 71, 130, 142, 175, 187, 195, 208, 212, 228, 238, 277, 283	
As$_7^+$	29, 69, 128, 132, 149, 161, 201, 204, 211, 228, 234, 306, 310	
As$_7^-$	84, 94, 134, 140, 150, 154, 181, 186, 188, 203, 213, 249, 260, 267	
As$_8$	71, 110, 129, 143, 149, 174, 177, 198, 205, 211, 216, 226, 231, 249, 275, 278	
As$_8^+$	23, 28, 48, 68, 69, 132, 171, 189, 192, 199, 214, 235, 243, 250, 299, 348	
As$_8^-$	44, 60, 73, 115, 122, 156, 187, 200, 204, 209, 217, 227, 230, 254, 272	
As$_9$	54, 57, 63, 81, 101, 127, 136, 153, 184, 192, 197, 207, 215, 219, 227, 238, 241, 272, 307	
As$_9^+$	24, 42, 77, 98, 156, 174, 187, 194, 210, 241, 261, 270, 296	
As$_9^-$	55, 63, 77, 99, 105, 128, 141, 151, 157, 187, 199, 207, 214, 220, 228, 235, 238, 251, 257, 291	
As$_{10}$	46, 55, 73, 82, 102, 112, 135, 139, 156, 157, 183, 197, 204, 211, 217, 221, 224, 229, 232, 236, 250, 270, 306	
As$_{10}^+$	14, 26, 52, 69, 72, 85, 123, 128, 132, 177, 182, 192, 200, 203, 210, 212, 228, 233, 247, 295, 302	
As$_{10}^-$	35, 54, 61, 74, 105, 108, 136, 138, 156, 182, 189, 206, 209, 213, 219, 223, 227, 230, 234, 257, 264	
As$_{11}$	43, 47, 60, 75, 78, 107, 134, 135, 153, 156, 182, 189, 196, 203, 208, 213, 218, 224, 226, 229, 237, 242, 246, 268, 280	
As$_{11}^+$	52, 66, 71, 99, 105, 127, 132, 135, 153, 167, 172, 189, 192, 195, 206, 209, 212, 218, 220, 227, 238, 240, 252, 260, 271, 276	
As$_{11}^-$	38, 42, 53, 74, 76, 108, 123, 134, 152, 157, 178, 187, 193, 205, 209, 213, 216, 230, 240, 245, 270, 292	
As$_{12}$	63, 69, 85, 99, 109, 137, 141, 177, 178, 184, 204, 212, 219, 224, 237, 248, 252	
As$_{12}^+$	19, 57, 60, 63, 79, 100, 108, 112, 119, 130, 138, 175, 178, 181, 182, 189, 201, 203, 210, 224, 228, 233, 248, 256, 262	
As$_{12}^-$	58, 62, 83, 88, 102, 121, 132, 157, 166, 170, 185, 190, 198, 211, 216, 222, 234, 270, 278	
As$_{13}$	27, 32, 38, 44, 67, 80, 88, 89, 102, 112, 137, 145, 147, 160, 167, 172, 177, 189, 192, 194, 204, 207, 215, 222, 230, 233, 236, 241, 245, 269, 296,	
As$_{13}^+$	24, 28, 36, 52, 68, 81, 85, 102, 105, 112, 124, 139, 149, 153, 160, 172, 180, 183, 189, 192, 195, 200, 205, 216, 220, 225, 228, 230, 235, 240, 248, 264, 296	
As$_{13}^-$	23, 31, 44, 68, 78, 84, 95, 113, 120, 133, 149, 155, 161, 174, 180, 183, 185, 188, 196, 204, 213, 220, 225, 228, 232, 238, 248, 252, 295	
As$_{14}$	25, 28, 45, 64, 73, 75, 103, 120, 124, 134, 144, 146, 153, 164, 184, 187, 191, 193, 204, 207, 217, 221, 230, 234, 239, 244, 246, 253, 267,	

Table 2 continued

Cluster	This theory	Experimental and other theory
As_{14}^{+}	11, 26, 36, 46, 58, 68, 69, 72, 106, 108, 120, 123, 127, 134, 145, 179, 180, 185, 191, 194, 199, 204, 205, 216, 217, 218, 225, 231, 234, 235, 239, 246, 247, 262, 269	
As_{14}^{-}	11, 24, 46, 57, 58, 68, 75, 89, 108, 123, 126, 136, 144, 153, 157, 173, 181, 196, 200, 206, 211, 214, 216, 219, 222, 223, 227, 229, 235, 239, 245, 248, 268, 276	
As_{15}	12, 19, 35, 47, 56, 73, 75, 93, 96, 100, 102, 129, 151, 160, 164, 165, 173, 181, 186, 190, 193, 198, 200, 203, 206, 215, 139, 220, 235, 247, 249, 252, 259, 268, 275, 297, 299	
As_{15}^{+}	14, 19, 30, 42, 45, 56, 71, 74, 91, 97, 101, 102, 126, 150, 160, 163, 165, 170, 180, 185, 191, 193, 197, 201, 204, 207, 211, 137, 222, 224, 230, 241, 243, 252, 258, 268, 275, 297	
As_{15}^{-}	23, 24, 39, 60, 61, 69, 72, 79, 103, 113, 116, 129, 137, 145, 147, 153, 164, 176, 181, 183, 188, 193, 194, 201, 202, 205, 221, 222, 224, 226, 230, 233, 238, 242, 248, 250, 253, 270	

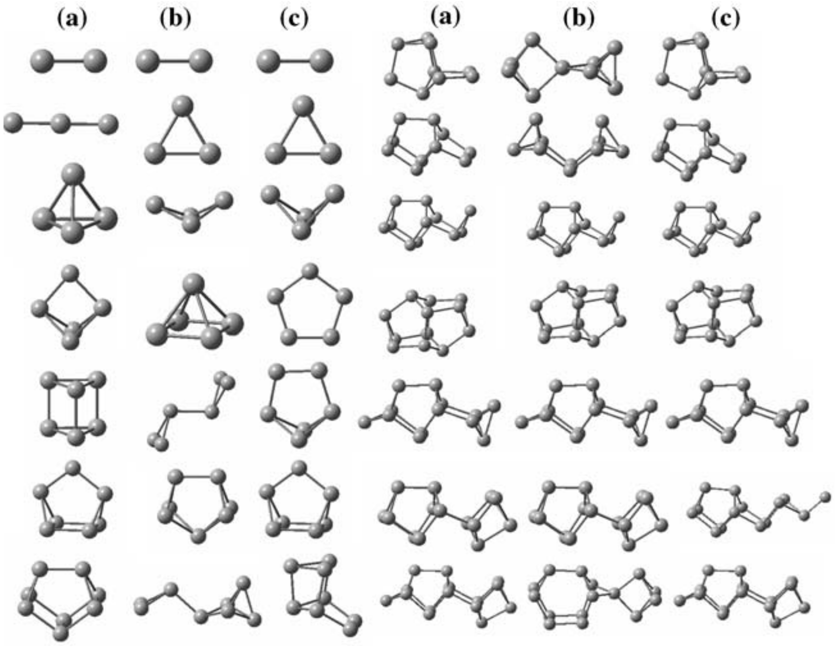

Fig. 1 Ground-state geometries of (**a**) neutral, (**b**) cationic, and (**c**) anionic arsenic clusters containing 2–15 atoms

energy difference of the two structures is 0.52 eV. The ground state of As_8^- is C_s ($^2A''$) in symmetry, which can be viewed as the ground-state structure of As_6 by adding two As atoms in one side. Assembling the stable structure of As_3^+ and As_5, we can obtain the lowest-energy structure of As_8^+ with C_s ($^2A'$) symmetry, which has different structure from its neutral and anion. The As_9 formed by a cuneane As_8 with a twofold atom added to the bottom bond. The lowest-energy structures we found for both As_9 and As_9^- are all with C_s symmetry, which may be viewed as a dimmer attached to the most stable form of As_7 and have been confirmed to be lower in energies with no imaginary frequencies. Adding two As atoms in the same side of cuneane As_8, we obtain the ground state of As_{10}, which has the same geometry as the anion. This structure is different from the previous work published on Ref. [23]. I also optimize their structure using the B3LYP/6-311 + G(d) level and found that my structure is the lowest energy structures. And the energy difference of the two structures is 0.57 eV. While cationic As_{10}^+ has the different structure from its neutral molecule with C_s ($^2A''$) symmetry. The ground-state structure of As_{11}^+ is the C_s ($^1A'$) form. The neutral and anionic As_{11} clusters have the same geometry with no bond forming between atom 1 and 7, which is different from the As_{11}^+. Both As_{12} and its charged clusters have the same D_{3d} structure, which can be seen as two cuneane As_8 binding with four same As atoms. Both As_{13} and its anion take the C_s structure as its ground state, while the structure has an imaginary frequency for the cationic As_{13} cluster. Relaxed the C_s structure and distorted it into new structure with lower C$_1$ symmetry, we can obtain the lowest-energy structure of cationic As$_{13}$. The most stable structure of As$_{14}$ is the C$_s$ (^{1}A′) form, which can be seen as the combination of As$_8$ and As$_6$ and has the same geometry as its cationic cluster. The anionic As$^-_{14}$, however, has the different structure as its neutral and cationic clusters. The optimized structure of neutral As$_{15}$ is with C$_s$ (^{2}A′) symmetry, which has the same geometry as its anion. Removing an electron from it produces the cationic As$^+_{15}$, which has the different structure as the neutral cluster although it is also with C$_s$ (^{1}A′) symmetry.

The structures of As$_2$, As$_3$, As$_4$, As$_5$, As$_6$, As$_8$, As$_{10}$, As$_{12}$, and As$_{14}$ in this work are the same as previous work published on Ref. [20]. And the structures of As$_2$, As$_4$, and As$_{12}$ in this work are also the same as previous work published on Ref. [2]. Other clusters are not discussed in their work.

Unlike in the bulk where the nearest-neighbor distance is well defined, the lack of a perfect structural symmetry in clusters makes it difficult to assign a unique nearest neighbor distance for each cluster. For example, the nearest-neighbor distance is easy to define in As$_2$, As$_3$, and As$_4$, as these clusters are symmetric. However, in As$_5$ and subsequent clusters the nearest-neighbor distances vary within a narrow range. For example, the 'nearest'-neighbor distances in As$_5$ range between 2.439 Å and 2.517 Å. We define an atom to be counted as a nearest neighbor if its distance is less than 2.600 Å. This cutoff was arrived at by examining all the interatomic distances in the clusters studied and by noting that there was a distinct gap in these distances beyond 2.600 Å. In As$_6$ to As$_{15}$, the nearest-neighbor distances lie in the range 2.503–2.552, 2.419–2.555, 2.458–2.563, 0.205–0.230, 2.278–2.521, 2.449–2.516, 2.477–2.516, 2.412–2.599, 2.451–2.567, and 2.471–2.567 Å, respectively. In Fig. 1 all bonds having lengths of 2.600 Å nm or less are connected.

In order to study the evolution of the nearest-neighbor distance, we have calculated the average nearest-neighbor distance by using the following expression:

$$\langle R \rangle = 1/n_{\mathrm{b}} \sum R_{ij}$$

Here R_{ij} is the distance between two atoms i and j with a cutoff = 2.600 Å and n_{b} is the total number of bonds between atoms that below this cutoff. The results are plotted in Fig. 2a. Note that with the exception of As$_6$ and As$_8$, the average nearest-neighbor distances generally increase with cluster size and reach the bulk limited of 2.49 Å [24] by the time the cluster contains five atoms. Thus, one can conclude that the evolution of the nearest-neighbor distance approaches the bulk value rather rapidly.

Unfortunate, the same cannot be said about the geometry. For example, the geometries in Fig. 1 do not resemble a fragment of the bulk arsenic structure [25]. This can also be viewed by studying the average coordination number. We define this by the following expression:

$$\mathrm{CN} = 1/n \sum N_i$$

Here N_i is the number of nearest-neighbor atoms surrounding the ith atom and the summation is carried over all the atoms with i ranging from 1 to n, the total number of atoms. The results are given in Fig. 2b. Note that there are marked changes in the coordination as a function of size. These occur at $n = 4$. The coordination numbers are small (~1.33) for $n = 2$ and 3 where the geometries are planar. At $n = 4$ the geometry becomes three-dimensional and the coordination number jumps from 1.33 to 3. This can also be seen from Fig. 1 by counting the number of bonds which increases from 2 to 6 as one goes from $n = 3$ to 4.

As the clusters are charged either by adding an electron or by removing one, their geometries are expected to undergo modifications. The average nearest-neighbor distances in charged clusters computed using Eq. 1 are compared with neutral clusters in Table 3. We note that these distances are generally different from those in neutral clusters for $n < 12$ and become equal from 12- to 15-atom clusters. This is as expected since, in a small cluster, removal or addition of a charge will create a bigger perturbation than in larger clusters.

Binding energy and relative stability

The relative stability of clusters can be studied through the measurement of the mass ion intensities. However,

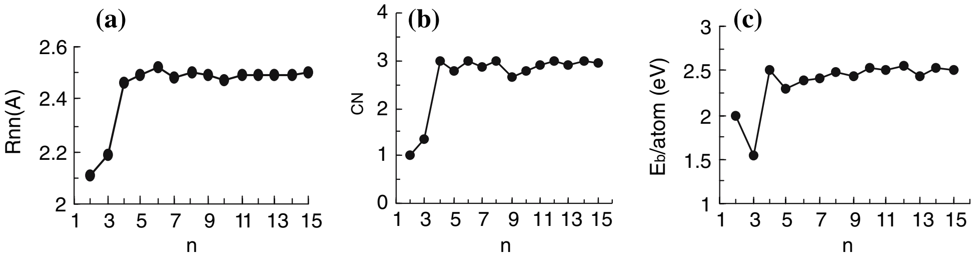

Fig. 2 (**a**) Average nearest-neighbor distance (**b**) coordination number, and (**c**) binding energy/atom as a function of size for neutral As$_n$ (n = 2–15) clusters

Table 3 Average nearest-neighbor distances (Å) of neutral, cationic, and anionic arsenic clusters

n	Neutral	Cation	Anion
2	2.111	2.114	2.211
3	2.189	2.356	2.425
4	2.463	2.474	2.469
5	2.494	2.523	2.343
6	2.519	2.427	2.464
7	2.481	2.507	2.481
8	2.497	2.476	2.481
9	2.494	2.498	2.457
10	2.474	2.488	2.478
11	2.487	2.506	2.489
12	2.490	2.491	2.506
13	2.490	2.396	2.494
14	2.495	2.498	2.493
15	2.499	2.505	2.497

interpretation of these results is not always unambiguous. Note that in mass spectroscopy experiments the clusters have to be ionized before their intensities can be measured. It is not entirely clear if the measured intensity distribution of the clusters represents the stability of the charged clusters or their neutral precursors. For example, if the mass spectra are collected after the ionized clusters have time to relax to their stable configuration, the corresponding mass-ion intensities could be different from the neutral precursors; one has to assume that the charged clusters are formed by single photon ionization and that there are no photo-induced fragmentations of the clusters in the process. These difficulties are manifested in experimental observations that differ from one group to another. An unambiguous insight into the relative stability of clusters can be gained by analyzing their energetic. We first calculate the binding energy/atom of neutral clusters. This is defined by

$$E_{\mathrm{b}} = -[E_n/n - E_0]$$

where E_n is the total energy of the neutral cluster (given in Table 1) containing *n*-atoms and E_0 is the energy of the atom. The binding energy/atom E_{b} is plotted as a function of cluster size in Fig. 2c. We note that the binding energy rises monotonically with cluster size and contains only a bump at $n = 3$ and 4. It is to be noted that binding energy seem to have a periodic step-like behavior, so that odd *n* values have lower energy gains when compared to even *n* values upon increasing *n*. This is an electronic effect since even *n* clusters are closed-shell systems with an even number of number, while odd *n* clusters have an odd number of electrons.

To study the relative stability, it is more instructive to analyze the first derivative of the total energy, i.e., the energy gain in adding an atom to an existing cluster. We first investigated this energy gain, hereafter referred to as stabilization energy, for neutral cationic and anionic clusters, namely

$$\begin{aligned}\Delta E_n^0 &= -[(E_n^0 - E_{n-1}^0) - E_0]\\ \Delta E_n^+ &= -[(E_n^+ - E_{n-1}^+) - E_0]\\ \Delta E_n^- &= -[(\Delta E_n^- - E_{n-1}^-) - E_0]\end{aligned}$$

These are plotted in Fig. 3a–c. E_n^0, E_n^+, and E_n^- correspond to the total energy of the neutral and charged *n*-atom cluster in its ground state, respectively. These energies are given in Table 1. From Fig. 3, we can see that the cluster size distributions exhibit strong even-odd alternations with several magic numbers. The neutral As$_n$ clusters are found to be even-numbered with local maxima at $n = 2$, 4, and 14, while the cationic and anionic clusters are preferentially odd-numbered with As$_3^+$, As$_5^+$, As$_7^+$, As$_2^-$, As$_5^-$, and As$_{15}^-$ being the most stable ions.

Electronic properties

The ionization potential measures the energy difference between the ground state of the neutral and the ionized clusters. If the ionized cluster has the same geometry as the ground state of the neutral, the ionization energy corresponds to the vertical ionization potential (VIP). On the other hand, the energy difference between the ground state of the cation and ground state of the neutral is referred to as the adiabatic ionization potential (AIP). Thus the vertical ionization potential is always larger than the adiabatic ionization potential and the energy difference between them is an indication of the energy gain due to structural relaxation. In the Fig. 4 we present the evolution of the

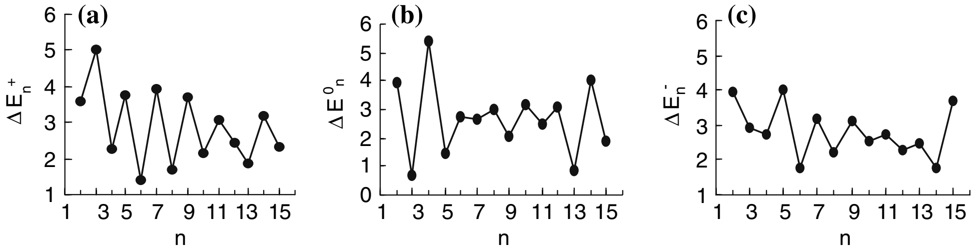

Fig. 3 Energy gain in adding an atom to a (**a**) positively charged cluster, ΔE_n^+, (**b**) neutral cluster, ΔE_n^0, and (**c**) negatively charged cluster, ΔE_n^-, for $2 \le n \le 15$

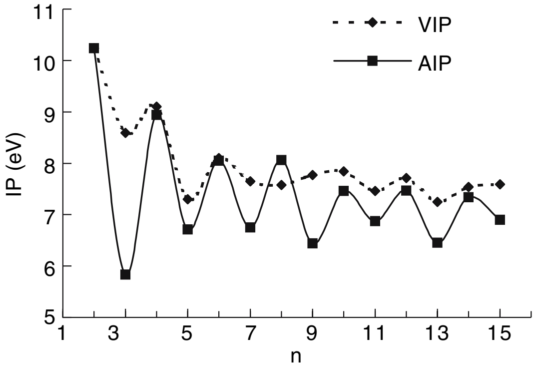

Fig. 4 Vertical ionization potential (VIP, dashed line) and adiabatic ionization potential (AIP, solid line) as a function of cluster size for arsenic clusters

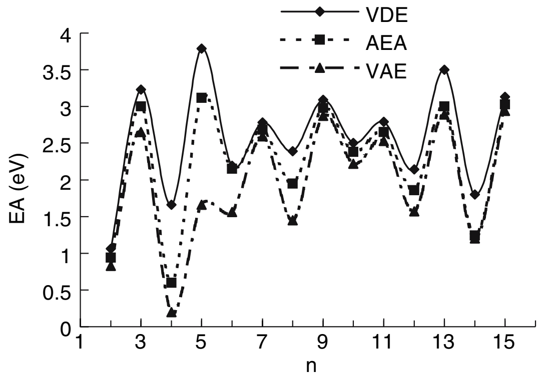

Fig. 5 Vertical detachment energy (VDE, solid line), adiabatic electron affinity (AEA, dashed line), and vertical attachment energy (VAE, dotted line) as a function of cluster size for arsenic clusters

ionization potential with the cluster size. There are three important features to be noted in the Fig. 4. First, the ionization potentials of clusters from $n = 3$ up to $n = 15$ are lower than that of the atom (9.87 eV). Second, there are odd-even alternations in the ionization potentials as a function of size with higher IP being associated with even-number cluster. The clusters with $n = 2$ and 4 show higher values for both AIP and VIP. Three, it is observed that the IP values have the tendency of decrease when the number of As units in the cluster increases.

Both vertical and adiabatic values for the electron affinity (EA) for the lowest energy isomers of the arsenic clusters were computed in this study. The vertical electron affinity (VEA, also called vertical detachment VDE) is the difference in the energy between the ground state of the anion and the energy of the neutral cluster having the anionic geometry. The adiabatic electron affinity (AEA), on the other hand, is the difference in the total energy between the ground state of the anion and the neutral cluster. The vertical attachment energy (VAE) has also been computed, defined as the energy difference between the neutral and anionic clusters with both at the neutral cluster optimized geometry. Although the vertical attachment energy is not currently measured through any experiment, it provides a lower bound to the AEA in the same way as the VDE is an upper bound to it. The calculated values of the above quantities for the As_n cluster are displayed in Fig. 5. Our calculated values agree satisfactorily with available photoemission experiments [4]. The measured maximum at $n = 5$ and the minima at $n = 2$ are all reproduced. The relative ordering of the VEA, AEA, and VAE is as expected. Particularly small values are exhibited by the symmetric clusters with $n = 4$, 6, 8, and 12.

The computed highest occupied molecular orbital (HOMO)-lowest unoccupied molecular orbital (LUMO) gap results for the neutral, positively charged, and negatively charged As clusters are depicted in Fig. 6a–c. Note that a cluster with a closed electronic shell is characterized by a large HOMO-LUMO gap. It also exhibits enhanced binding energy compared to their neighbors. We see from Fig. 6a that the HOMO-LUMO gaps for neutral clusters exhibit odd-even alteration with even-atom clusters having larger HOMO-LUMO gaps than odd-atoms clusters. And the HOMO-LUMO gaps in neutral clusters are particularly large for As_2, As_4, and As_{12}. The peak in As_4 is easily understood in the jellium models as the cluster would contain 20 valence electrons, just enough for electronic shell closure. While none of As_2 and As_{12} clusters contain the number of valence electrons necessary to form closed electronic shells in a jellium model as describe earlier. We see from Fig. 3b that the energy gain, ΔE_n^0 shows a peak for all of these three clusters.

Fig. 6 HOMO-LUMO gap of (**a**) neutral, (**b**) negatively charged, and (**c**) positively charged clusters

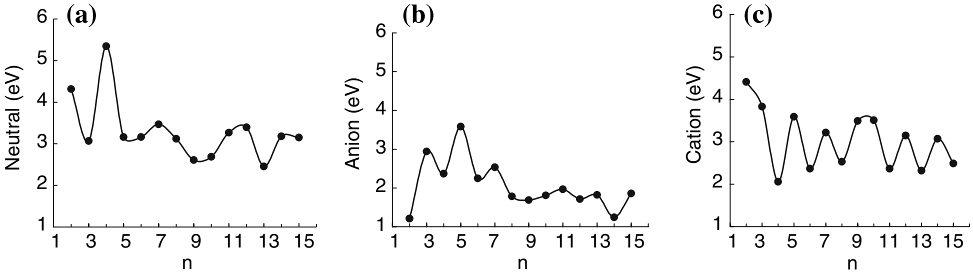

The situation is somewhat different for charged clusters. The HOMO-LUMO gaps for charged clusters also exhibit odd-even alteration. But clusters with odd atoms have larger HOMO-LUMO gaps than clusters with even atoms. For negatively charged clusters (see Fig. 6b) conspicuous peaks in the HOMO-LUMO gaps do exist for As_3^- and As_5^-. Note that although As_5^- do not accord the jellium model, it is consistent with the relative stability as seen from the systematic inΔE_n^- in Fig. 3c. However, the large HOMO-LUMO gaps in As_3^-, is neither consistent with the electronic shell closure nor with their relative stabilities. For positively charged arsenic clusters, the As_2^+, As_3^+, As_5^+, and As_9^+ have particular stabilities. We see from Fig. 3a thatΔE_n^+ for As_3^+, As_5^+ and As_9^+ are large and thus the large HOMO-LUMO gaps are consistent with their enhanced stabilities. Of particular interest is the peak at As_3^+. If arsenic in As_3 can be regarded as three-valent, As_3^+ would have eight valence electrons and hence has a very large HOMO-LUMO gap. However, the large HOMO-LUMO gaps in As_2^+, is neither consistent with the electronic shell closure nor with their relative stabilities.

Conclusion

We have presented a comprehensive DFT-B3LYP study for arsenic cluster neutral, cations, and anions in the size of $n = 2$–15. The total energies of these clusters are used to study the evolution of their binding energy, relative stability, ionization potentials, and electron affinities as a function of size. The results can be summarized as follows: (1) The nearest-neighbor distances and coordination numbers undergo a significant jump when the cluster changes from two to three dimensions. (2) The binding energy/atom evolve monotonically for neutral clusters. It has a periodic step-like behavior, so that odd n values have lower energy gains when compared to even n values upon increasing n. (3) The energy gain, ΔE_n exhibits strong even-odd alternations with several magic numbers. The neutral As_n clusters are found to be even-numbered with local maxima at $n = 2$, 4, and 14, while the cationic and anionic clusters are preferentially odd-numbered with As_3^+, As_5^+, As_7^+, As_2^-, As_5^-, and As_{15}^- being the most stable ions. (4) Ionization potential has the tendency of decrease when the number of As units in the cluster increases. The clusters with $n = 2$ and 4 show higher IP values, while particularly small EA values are exhibited by the symmetric clusters with $n = 4$, 6, 8, and 12. Our calculated values agree satisfactorily with available photoemission experiments. The measured maximum at $n = 5$ and the minima at $n = 2$ are all reproduced. The relative ordering of the VEA, AEA, and VAE is as expected. (5) The HOMO-LUMO gaps for both neutral and charged clusters exhibit odd-even alteration. HOMO-LUMO gaps for neutral clusters exhibit even-atom clusters having larger HOMO-LUMO gaps than odd-atoms clusters with particularly large values for As_2, As_4, and As_{12}. While HOMO-LUMO gaps for charged clusters show reversing results with As_3^-, As_5^-, As_2^+, As_3^+, As_5^+, and As_9^+ having particularly large values.

Acknowledgements This work was financially supported by the National Natural Science Foundation of China (Grant No. 20603021), Youth Foundation of Shanxi (2007021009) and the Youth Academic Leader of Shanxi.

References

1. Ballone P, Jones RO (1994) J Chem Phys 100:4941
2. Shen M, Schaefer III (1994) J Chem Phys 101:2261
3. Yoo RK, Ruscic B, Berkowitz J (1992) J Chem Phys 96:6696
4. Lippa TP, Xu SJ, Lyapustina SA (1998) J Chem Phys 109:10727
5. Chi X, Tian S, Xu K (2002) Chin J Chem Phys 15:22
6. Jones RO, Ganteor G, Hunsicker S, Pieperhoff P (1995) J Chem Phys 103:9549
7. Polak ML, Joe Ho, Gustav G, Lineberger WC (1992) J Chem Phys 97:8990
8. Zhang H, Balasubramanian K (1992) J Chem Phys 97:3437
9. Igel-Mann G, Stoll H, Preuss H (1993) Mol Phys 80:325
10. Haser M, Schneide U, Ahlrichs R (1992) J Am Chem Soc 114:9551
11. Scherer OJ (1990) Angew Chem Int Ed Engl 102:1137
12. Dimaio AJ, Rheingold AL (1990) Chem Rev 90:169
13. Voako SH, Wilk L, Nusair M (1980) Can J Phys 58:1200
14. Lee C, Yang W, Parr RG (1988) Phys Rev B 37:785
15. Beck AD (1993) J Chem Phys 98:5468
16. Knight WD, Clemenger K, Saunders WA, Chou MY, Cohen ML (1984) Phys Rev Lett 52:2141
17. Rao BK, Jena P (1985) Phys Rev B 32:2058
18. Bhasker ND, Frueholz RP, Klimeak CM, Cook RA (1987) Phys Rev B 36:4418
19. Frisch MJ, Trucks GW, Schlegel HB, Scuseria GE, Robb MA, Cheeseman JR, Zakrzewski VG, Montgomery JA, Stratmann RE, Burant JC, Dapprich S, Millam JM, Daniels AD, Kudin KN, Strain MC, Farkas O, Tomasi J, Barone V, Cossi M, Cammi R, Mennucci B, Pomelli C, Adamo C, Clifford S, Ochterski J, Petersson GA, Ayala PY, Cui Q, Morokuma K, Malick DK, Rabuck AD, Raghava-chari K, Foresman JB, Cioslowski J, Ortiz JV, Stefanov BB, Liu G, Liashenko A, Piskorz P, Komaromi I, Gomperts R, Martin RL, Fox DJ, Keith T, Al-Laham MA, Peng CY, Nanayakkara A, Gonzalez C, Challacombe M, Gill PMW, Johnson B, Chen W, Wong MW, Andres JL, Gonzalez C, Head-Gordon M, Replogle ES, Pople JA (1998) computer code GAUSSIAN98, revision A.6. Gaussian, Inc., Pittsburgh, PA
20. Zhao J, Zhou X, Chen X, Wang J, Jellinek J (2006) Phys Rev B 73:115418
21. Bosworth YM, Clark JH, Rippon DM (1973) J Mol Spectrosc 46:240
22. Huber KP, Herzberg G (1979) Molecular spectra and molecular structure IV constants of diatomic molecules. Van Nostrand Reinhold, New York
23. Yi J (2000) Chem Phys Lett 325:269
24. Lide DR (ed) (2000). In: Chemical rubber company handbook of chemistry and physics, 81st edn. CRC Press, Boca Raton, Florida, USA
25. Schiferl D, Barrett CS (1969) J Appl Crystallogr 2:30